Biosensors and Bioelectronics 100 (2018) 326–332

Contents lists available at ScienceDirect

Biosensors and Bioelectronics

journal homepage: www.elsevier.com/locate/bios

Enzymatic logic calculation systems based on solid-state electrochemiluminescence and molecularly imprinted polymer film electrodes

Wenjing Lian[a,b], Jiying Liang[a], Li Shen[c], Yue Jin[d], Hongyun Liu[a,*]

[a] College of Chemistry, Beijing Normal University, Beijing 100875, People's Republic of China
[b] Department of Applied Chemistry, College of Basic Science, Tianjin Agricultural University, Tianjin 300384, People's Republic of China
[c] Logistics School, Beijing Wuzi University, Beijing 101149, People's Republic of China
[d] Institute of Apicultural Research, Chinese Academy of Agricultural Sciences, Beijing 100093, People's Republic of China

ARTICLE INFO

Keywords:
Biomacromolecular logic gates
Molecularly imprinted polymer films
Electrochemiluminescence
Multi-valued outputs
Glucose oxidase

ABSTRACT

The molecularly imprinted polymer (MIP) films were electropolymerized on the surface of Au electrodes with luminol and pyrrole (PY) as the two monomers and ampicillin (AM) as the template molecule. The electrochemiluminescence (ECL) intensity peak of polyluminol (PL) of the AM-free MIP films at 0.7 V vs Ag/AgCl could be greatly enhanced by AM rebinding. In addition, the ECL signals of the MIP films could also be enhanced by the addition of glucose oxidase (GOD)/glucose and/or ferrocenedicarboxylic acid ($Fc(COOH)_2$) in the testing solution. Moreover, $Fc(COOH)_2$ exhibited cyclic voltammetric (CV) response at the AM-free MIP film electrodes. Based on these results, a binary 3-input/6-output biomolecular logic gate system was established with AM, GOD and $Fc(COOH)_2$ as inputs and the ECL responses at different levels and CV signal as outputs. Some functional non-Boolean logic devices such as an encoder, a decoder and a demultiplexer were also constructed on the same platform. Particularly, on the basis of the same system, a ternary AND logic gate was established. The present work combined MIP film electrodes, the solid-state ECL, and the enzymatic reaction together, and various types of biomolecular logic circuits and devices were developed, which opened a novel avenue to construct more complicated bio-logic gate systems.

1. Introduction

Molecular logic gates, similar to their electronic counterparts based on silicon-based integrated circuits, can perform various computations but at the molecular level (Andreasson and Pischel, 2015; de Silva and Uchiyama, 2007; de Silva et al., 1993; Stojanovic et al., 2002; Xia et al., 2010). Biomolecular logic gates are a type of molecular logic gates that employ biomaterials or biomolecules such as nucleic acids (DNA), enzymes or proteins to construct the basic molecular devices (Katz, 2015; Willner et al., 2008). In recent years, biomolecular logic gates have attracted increasing attentions from researchers due to their high application potential in different fields including diagnostics, sensing and molecular recognition (Gui et al., 2014; Ling et al., 2015; Park et al., 2010).

One great challenge in developing biomolecular logic gates is to increase the complexity of the system, so that more complicated calculations can be accomplished. One direction in this regard is to increase the number of input and/or output of the logic gates. Early bio-logic gate system had only one or two inputs/outputs (Manesh et al., 2009; Privman et al., 2009). Afterwards, biomolecular logic devices with multiple inputs/outputs were constructed (Erbas-Cakmak et al., 2013; Guz et al., 2014; He et al., 2014; Liu et al., 2015a, 2015b; Shi et al., 2015). The second direction is to develop non-Boolean logic devices. Compared with the traditional Boolean logic gates, the non-Boolean logic devices such as encoder/decoder, multiplexer/demultiplexer and keypad lock can accomplish some special and specific tasks (Gao et al., 2017). The third direction in increasing the complexity is to develop multi-valued logic gates (Ran et al., 2014). Usually, the logic gate system is binary, i.e. it has only two states in its input/output: on and off, or true and false. The disadvantage of binary logic gates is their uncertainty and imprecision especially when more complicated information needs to be processed. Multi-valued logic gate system can make up the imperfection. It involves switches between more than two states, and the increase of the number of states in input/output brings about higher data storage densities and more powerful information processing capability (He et al., 2015). However, only a few studies

* Corresponding author.
E-mail address: liuhongyun@bnu.edu.cn (H. Liu).

http://dx.doi.org/10.1016/j.bios.2017.09.023
Received 27 July 2017; Received in revised form 13 September 2017; Accepted 14 September 2017
Available online 18 September 2017
0956-5663/

have been reported on the multi-valued logic gates based on biomolecular system until now (He et al., 2015; Pu et al., 2011; Ran et al., 2014).

Electrochemiluminescence (ECL), also referred to as electrogenerated chemiluminescence, is chemiluminescence triggered by electrochemical reactions (Hu and Xu, 2010), which demonstrates some unique advantages such as rapid response, low cost, high sensitivity, and simplified setup (Chen et al., 2014). Usually, cyclic voltammetry (CV) and ECL signals can be measured and obtained simultaneously by ECL instruments. Up to now, however, only a few investigations have been reported by our group on biomolecular logic gates with simultaneous CV and ECL responses as two types of outputs (Lian et al. 2015; Liu at al. 2015b).

The molecular imprinting technology is an approach that uses synthetic molecular imprinted polymer (MIP) with specific binding sites to recognize the target molecule (Chen et al., 2011). With the intrinsic advantages such as high selectivity, good mechanical strength, low cost, and easy preparation, MIP has been successfully applied as the recognition element in quantitative analysis (Erdossy et al., 2017; Kim et al., 2017; Moon et al., 2017; Chantada-Vazquez et al., 2016; Tan-Phat et al., 2013; Ton et al., 2015). Recently, MIP electrochemical and MIP-ECL sensors for the detection of various substances have been developed, which combine the excellent selectivity of MIP and the high detection sensitivity of voltammetry and ECL (Li et al., 2012; Wu et al., 2012; Xue et al., 2014). However, until now, very few reports have been made on the logic gate system on the basis of combination of MIP and ECL (Lian et al., 2015).

In the present work, a series of binary biomacromolecular logic gates and devices, and a ternary logic gate were developed based on the MIP films at electrodes and the solid-state ECL. The solid-state ECL, by immobilizing the ECL reagent on the electrode surface, usually demonstrates advantages over the solution-state ECL in its better signal-to-noise ratio, less consumption of ECL reagent, and simplified experimental design (Fu et al., 2016; Wang et al., 2014). Herein, the ECL reagent luminol and functional monomer pyrrole (PY) were electropolymerized into copolymer MIP films at the surface of electrodes with ampicillin (AM) as the template, designated as AM-PPY/PL MIP (PPY = polypyrrole and PL = polyluminol). AM is a type of β-lactam antibiotics, and is widely used for the treatment of infections in humans and animals (S. Wei et al., 2014). Under aerobic and basic conditions, β-lactam antibiotics such as AM can produce superoxide anion free radical ($O_2^{-\bullet}$) (Kubo et al., 1999), which was used in this work to oxidize PL and enhance its ECL signal. Thus, the ECL response of AM-PPY/PL MIP film system was employed to recognize and detect AM in its rebinding solution (Scheme 1A). On the other hand, the addition of glucose oxidase (GOD)/glucose and/or ferrocenedicarboxylic acid (Fc(COOH)$_2$) in the testing solution could improve the ECL intensity of the system. In addition, Fc(COOH)$_2$ also functioned as the electroactive probe and exhibited CV signal at the AM-free MIP film electrodes. Thus, with AM, GOD and Fc(COOH)$_2$ as inputs, and the corresponding CV and ECL responses as outputs, a binary 3-input/6-output logic gate was established. In addition, some non-Boolean logic devices, including an encoder, a decoder and a demultiplexer, were also constructed based on the same MIP system with elaborate designs. Especially, a ternary AND logic gate was successfully developed on the same platform. To the best of our knowledge, this is the first report on biomolecular multi-valued logic gate based on MIP and ECL. The present system combined MIP and solid-state ECL with the enzymatic reaction, demonstrating great potential in biocomputing. This new idea had generality to some extent, and might become a foundation for the development of some novel and more complicated biomolecular computing devices.

2. Experimental section

2.1. Preparation of MIP film electrodes

MIP films were fabricated on the surface of Au electrode by electropolymerization. First, the Au electrodes were sequentially polished with 1.0, 0.5 and 0.05 μm γ-alumina on chamois leathers to obtain a mirror-like surface, followed by ultrasonication in ethanol and water for 5 min, respectively. After optimization, the electropolymerization of AM-PPY/PL MIP films was performed by 5 cycles of CV scans at Au electrodes between 0 and 1.0 V at 50 mV s^{-1} in the solution containing 60 mM AM template, 20 mM PY and 5 mM luminol monomers in 0.1 M phosphate buffer solutions at pH 6.0. AM-free MIP films were prepared by placing the MIP film electrodes in 20 mL methanol/acetic acid (9:1, v/v) solutions for 20 min with magnetic stirring so that the AM molecules previously entrapped in the MIP films could be removed. The AM-free MIP film electrodes were then rinsed with water and dried at room temperature. The AM-rebinding MIP film electrodes were formed by incubation of the AM-free MIP film electrodes in 0.1 M phosphate buffer solutions at pH 7.0 containing different concentrations of AM for 15 min, followed by water rinsing and room temperature drying.

The PL, AM-PL and non-molecularly imprinted polymer (NIP) film electrodes were prepared with the similar method.

The reagents and apparatus used in this work, and the characterization of AM-PPY/PL MIP films, were described in details in Supplementary information.

3. Results and discussion

3.1. Molecular recognition of AM by MIP films

The simultaneous CV and ECL experiments were performed to confirm the molecular recognition function of the MIP films toward AM (Fig. 1). In pH 8.0 blank buffers, a CV oxidation peak at approximate

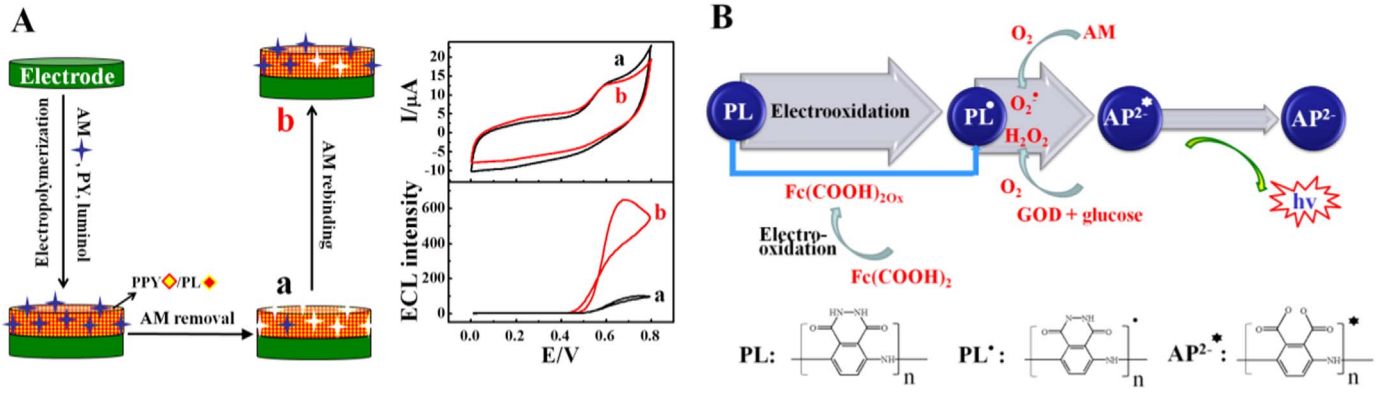

Scheme 1. Schematic representation of (A) the fabrication process of AM-PPY/PL MIP film electrodes and (B) the possible mechanism of ECL signals controlled by AM, GOD/glucose and Fc(COOH)$_2$.

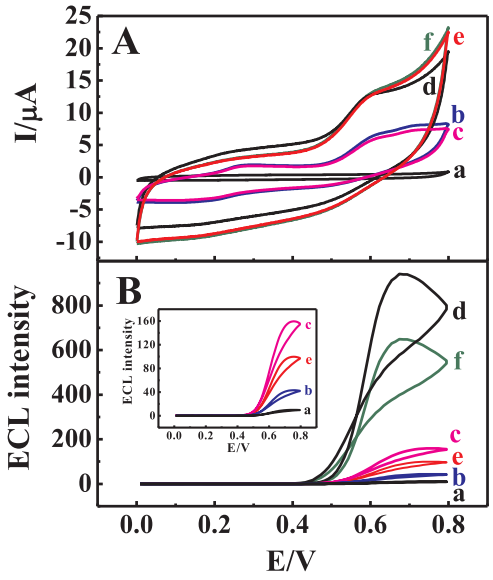

Fig. 1. (A) CV and (B) ECL signals at 0.05 V s^{-1} in pH 8.0 buffers equilibrated with air at (a) bare Au electrodes, (b) PL, (c) AM-PL, (d) AM-PL/PPY MIP, and (e) AM-free MIP film electrodes, and (f) AM-rebinding MIP film electrodes after 50 μM AM rebinding. Inset: magnification of the ECL signals for curves a–c, and e.

0.6 V vs Ag/AgCl was observed at PL and AM-PL film electrodes, respectively (Fig. 1A, curves b and c), which should be attributed to the oxidation of PL (X. Wei et al., 2014. At AM-PPY/PL MIP film electrodes, the CV oxidation peak at 0.6 V increased significantly (Fig. 1A, curve d) because of the good conductivity of PPY (Sadki et al., 2000). At the AM-free and AM-rebinding MIP film electrodes, the CV peak height and shape showed no obvious change (Fig. 1A, curves e and f), since this peak originated from PL and had nothing to do with AM.

In pH 8.0 buffers, a very small ECL peak at 0.7 V was observed for PL films (Fig. 1B, curve b), and this ECL peak increased for AM-PL films (Fig. 1B, curve c). The mechanism of AM enhancement for the ECL of PL was described in Scheme 1B (Kubo et al., 1999). The dissolved oxygen in solution can be oxidized by AM in the films and become superoxide anion free radical ($O_2^{-\bullet}$) under aerobic and alkaline conditions. The $PL^{\bullet}$, the product of electrochemical oxidation of PL, can then react with $O_2^{-\bullet}$ and become the intermediate at the excited state, known as AP^{2-}*, which can emit the enhanced ECL signal (X. Wei et al., 2014. The ECL response could be further increased at AM-PL/PPY MIP film electrodes due to the good conductivity of PPY (Fig. 1B, curve d) (Sadki et al., 2000). In comparison, for the AM-free MIP films, the ECL peak at 0.7 V decreased significantly (Fig. 1B, curve e), because the AM molecules previously entrapped in the MIP films were now removed. For AM-rebinding MIP films, the ECL peak increased again (Fig. 1B, curve f) due to the rebinding of AM molecules in the MIP films. The increase in ECL peak for AM-rebinding MIP films in comparison with that for AM-free MIP films was dependent on the concentration of AM (C_{AM}) in the rebinding solution (Supplementary information Fig. S4). All these results indicate that the MIP films have a specific recognition function toward AM, and AM in the MIP films can enhance the ECL response of PL effectively.

The results of electrochemical impedance spectroscopy (EIS) of $Fe(CN)_6^{4-/3-}$ also confirmed that AM could be recognized by the MIP films (Supplementary information Fig. S5). The detailed discussion on the EIS results is provided in Supplementary information.

In contrast, at the NIP film electrodes, both CV and ECL responses demonstrated no change with the same removal and rebinding steps (Supplementary information Fig. S6). This is understandable because there is no AM template in the NIP films, and NIP films thus have no recognition function toward AM.

3.2. AM- and O_2-sensitive ECL switching behaviors for MIP films

Based on the ECL results demonstrated above, AM could be used as a stimulus to trigger the ECL signal for the MIP film system. After the rebinding of 50 μM AM under aerobic conditions, the AM-rebinding MIP film electrodes showed a much larger ECL peak at 0.7 V than the AM-free MIP film electrodes (Fig. 1B, curves e and f). By defining the ECL peak intensity at the AM-free MIP film electrodes as the off state and that at AM-rebinding MIP film electrodes as the on state, the AM-sensitive ECL on-off behavior was observed and could be reversibly

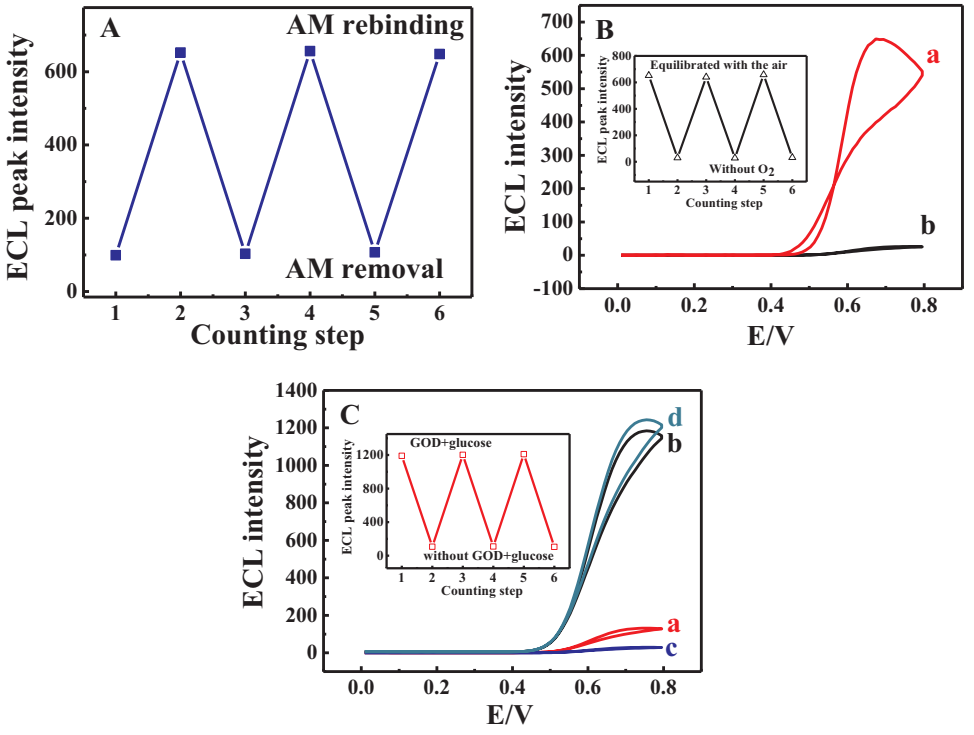

Fig. 2. (A) Dependence of ECL peak intensity at 0.7 V for MIP film electrodes on the switch between AM removal and 50 μM AM rebinding in pH 8.0 buffers equilibrated with air. (B) ECL responses at AM-rebinding MIP film electrodes after 50 μM AM rebinding in pH 8.0 buffers (a) equilibrated with air and (b) in the absence of O_2. Inset in B: dependence of ECL peak intensity at 0.7 V at AM-rebinding MIP film electrodes on the switch of equilibrated with air and in the absence of O_2 in pH 8.0 buffers. (C) ECL signals of AM-free MIP film electrodes in pH 8.0 buffers (a) in the presence of O_2, (b) in the presence of O_2 with addition of 1 mg mL^{-1} GOD and 2 μM glucose, (c) in the absence of O_2 with addition of GOD and glucose, and (d) in the absence of O_2 with addition of 2 μM H_2O_2. Inset in C: dependence of ECL peak intensity at 0.7 V at AM-free MIP film electrodes in pH 8.0 buffers equilibrated with air on the switch between with and without GOD/glucose.

repeated at least 3 cycles by switching the MIP film electrodes between AM removal and rebinding (Fig. 2A).

In addition, the influence of O_2 on the ECL response of the AM-rebinding MIP film electrodes was also explored (Fig. 2B). Before ECL tests, the high-purity nitrogen was bubbled into the pH 8.0 buffers in the cell for more than 15 min, and a nitrogen atmosphere was then maintained during the whole experiment. In this case, the ECL peak at 0.7 V for the AM-rebinding MIP films was much smaller than that in the presence of O_2 (Fig. 2B, curves a and b), because the oxygen is necessary in producing the high ECL signal (Scheme 1B) (Kubo et al., 1999). In the absence of oxygen, $O_2^{-\bullet}$ could not be produced, and AP^{2-}* could not be formed. If the ECL peak at 0.7 V at the AM-rebinding MIP film electrodes in the presence of oxygen was defined as the on state and that in the absence of oxygen as the off state, by switching the AM-rebinding MIP film electrodes in the buffer solutions between with and without O_2, the reversible ECL on-off behavior was clearly observed (Fig. 2B, Inset). In contrast, the CV response of AM-rebinding MIP film electrodes was not sensitive to dissolved oxygen in pH 8.0 buffers (Supplementary information Fig. S7, curves a and b).

3.3. GOD/glucose-sensitive ECL switching behaviors for AM-free MIP films

After the addition of GOD and glucose in pH 8.0 buffers equilibrated with air, the ECL peak at 0.7 V for AM-free MIP films was significantly enhanced (Fig. 2C, curve b) in comparison with that in the absence of GOD/glucose (Fig. 2C, curve a). This is because the reaction between glucose and oxygen can be catalyzed by GOD, and H_2O_2 is thus produced (Yao and Hu, 2009). H_2O_2 can then oxidize $PL^{\bullet}$ into AP^{2-}* and therefore enhance the ECL peak intensity (Scheme 1B) (X. Wei et al., 2014). This mechanism was further supported by the comparative experiments. The direct addition of H_2O_2 in N_2-saturated solution showed the similar enhancement in ECL response to the addition of GOD/glucose in air-equilibrated solution (Fig. 2C, curves d and a). But under the nitrogen atmosphere, the ECL peak intensity of the system was quite small even with the addition of GOD/glucose (Fig. 2C, curve c). Thus, GOD/glucose could be used as a stimulus to switch the ECL intensity of the system. As shown in Fig. 2C Inset, the reversible ECL on-off behavior was observed by switching the AM-free MIP film electrode in the buffer solutions between with and without the addition of GOD/glucose.

3.4. $Fc(COOH)_2$-sensitive CV and ECL switching behaviors for AM-free MIP films

$Fc(COOH)_2$ is an electroactive probe (Yao and Hu, 2009) and also an efficient promoter for the ECL signal of luminol in solution (Sato et al., 2001, 2005). After the addition of $Fc(COOH)_2$ in the buffer solution containing GOD and glucose in the presence of O_2, the CV oxidation peak current at about 0.6 V was increased obviously at the AM-free MIP film electrodes (Fig. 3A, curve b), which should be attributed to the contribution of both $Fc(COOH)_2$ and PL (Supplementary information Fig. S8). However, For AM-rebinding MIP films under the same condition, the oxidation peak became smaller (Fig. 3A, curve d), and the peak height was at the same level as that for AM-rebinding MIP films without $Fc(COOH)_2$ (Fig. 3A, curve c). This is because most of the vacant recognition sites in the AM-free MIP films are occupied again by AM molecules after the rebinding, making the diffusion of $Fc(COOH)_2$ molecules through the films and their approach to the electrode surface become very difficult.

After the addition of $Fc(COOH)_2$ in the buffer containing GOD and glucose in the presence of oxygen, the ECL peak at about 0.7 V at AM-free MIP film electrodes was also enhanced apparently (Fig. 3B, curve b), which should be attributed to the additional oxidation of PL into $PL^{\bullet}$ by $Fc(COOH)_{2Ox}$, the product of electrochemical oxidation of $Fc(COOH)_2$ (Scheme 1B) (Sato et al., 2001, 2005). At AM-rebinding MIP film electrodes, the enhancement of ECL peak by $Fc(COOH)_2$ was also observed (Fig. 3B, curve d). The contribution from AM, $Fc(COOH)_2$ and GOD/glucose led to the ECL peak larger than that with the contribution only from $Fc(COOH)_2$ and AM (Fig. 3B, curve c) or only from $Fc(COOH)_2$ and GOD/glucose (Fig. 3B, curve b). $Fc(COOH)_2$ could thus be used as a stimulus in the $Fc(COOH)_2$-sensitive CV and ECL on-off experiments for the system. For example, by switching AM-free MIP film electrodes in the buffer containing GOD and glucose between with and without $Fc(COOH)_2$, the reversible CV and ECL on-off behaviors were observed (Fig. 3C and D).

3.5. A binary 3-input/6-output logic circuit based on CV and ECL responses of the system

Basic binary logic gates are the foundation in the development of advanced and more complicated biomolecular logic devices. According to the above results for the system, a binary 3-input/6-output logic gate was constructed by defining AM, GOD and $Fc(COOH)_2$ as Inputs A, B and C, respectively, and the ECL peak responses at 5 different levels and the CV I_{pa} at 0.6 V as the 6 outputs. The definitions of the inputs and outputs are demonstrated in Scheme 2 and Supplementary information Table S2. Herein, the AM-free MIP film electrode in pH 8.0 buffers containing 2 μM glucose under aerobic condition was acted as the working platform.

All 8 possible combinations of the 3 inputs and the corresponding outputs are shown in Fig. 4. The input combinations (0,0,0) and (0,0,1) led to the smallest ECL response or the "1" state of Output E_1 (ECL ≤ 400) due to the absence of AM in the films and GOD in solution (Fig. 4A). The input combinations (1,0,0) and (1,0,1) resulted in the "1" state of Output E_2 (400 < ECL ≤ 1000) mainly because the presence of AM in the films amplified the ECL signal. The input combination (0,1,0) exclusively resulted in the "1" state of Output E_3 (1000 < ECL ≤ 1500) since the presence of GOD in solution triggered the enzymatic reaction and then led to the amplification of ECL response. The input combinations (0,1,1) and (1,1,0) led to the "1" state of Output E_4 (1500 < ECL ≤ 2500) due to the synergetic enhancement effect of GOD/$Fc(COOH)_2$ and GOD/AM, respectively. The input combination (1,1,1) exclusively resulted in the largest ECL response or the "1" state of Output E_5 (ECL > 2500) because of the synergetic enhancement effect of 3 inputs (AM, GOD and $Fc(COOH)_2$). It should be noted that the definition of thresholds for ECL signals was not arbitrary but based on the mechanism. For Output I, only the 2 input combinations (0,0,1) and (0,1,1) resulted in the "1" state, while the 6 others led to the "0" state (Fig. 4B). This is because only $Fc(COOH)_2$ at AM-free MIP film electrodes can display the increased CV oxidation peak at 0.6 V. According to these results, a truth table was established (Supplementary information Table S3), and the corresponding 3-input/6-output logic gate system was constructed (Fig. 4C), which is the combination of NOR, INHIBIT, AND and XOR gates.

3.6. A 1-to-2 demultiplexer and other logic devices based on the same system

Based on the same MIP film electrode system, various functional non-Boolean logic devices such as an encoder (Supplementary information Fig. S9), a decoder (Supplementary information Fig. S10) and a demultiplexer (Fig. 4D, E and Supplementary information Fig. S11) were constructed. The detailed discussion on establishment of the encoder and decoder is presented in Supplementary information. Herein, only the development of 1-to-2 demultiplexer is discussed. In electronics, a demultiplexer is a device that takes a single or small number of input signals and switches them between multiple output signals (Erbas-Cakmak et al., 2013). For example, the operation of forwarding one input signal into two different output channels can be accomplished by a 1-to-2 demultiplexer. Unlike the decoder, however, the demultiplexer needs the additional address input that selects either output channel to be used to take the input signal. The present system could

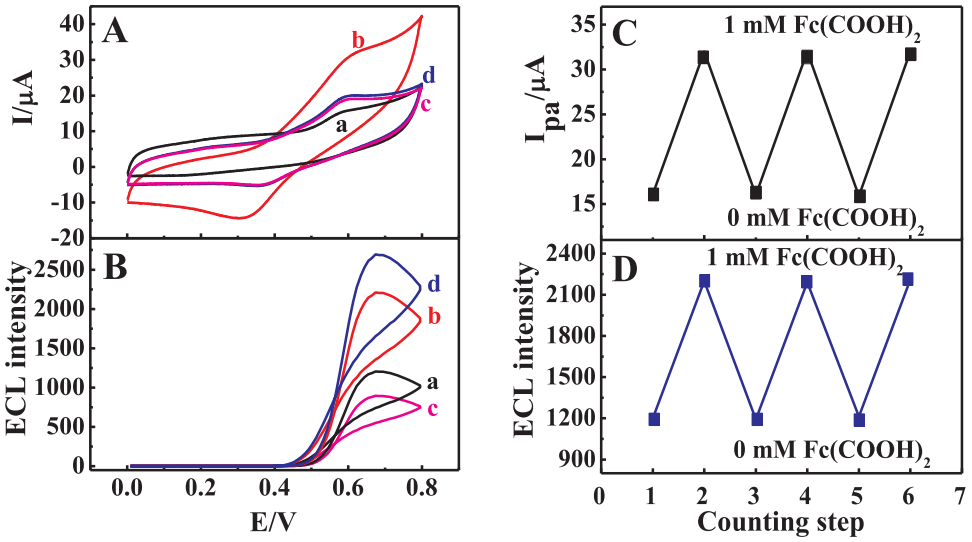

Fig. 3. (A) CV and (B) ECL response curves at (a) AM-free MIP film electrodes with GOD and glucose in solution, (b) AM-free MIP film electrodes with Fc(COOH)$_2$, GOD and glucose in solution, (c) AM-rebinding MIP film electrodes after 50 μM AM rebinding with Fc(COOH)$_2$ in solution, and (d) AM-rebinding MIP film electrodes after 50 μM AM rebinding with Fc(COOH)$_2$, GOD and glucose in solution. Dependence of (C) CV I_{pa} at 0.6 V and (D) ECL peak at 0.7 V at AM-free MIP film electrodes with GOD and glucose in solution on the switch between with and without Fc(COOH)$_2$. The concentrations of Fc(COOH)$_2$, GOD and glucose were 1 mM, 1 mg mL^{-1} and 2 μM, respectively. All solutions were pH 8.0 buffers equilibrated with air.

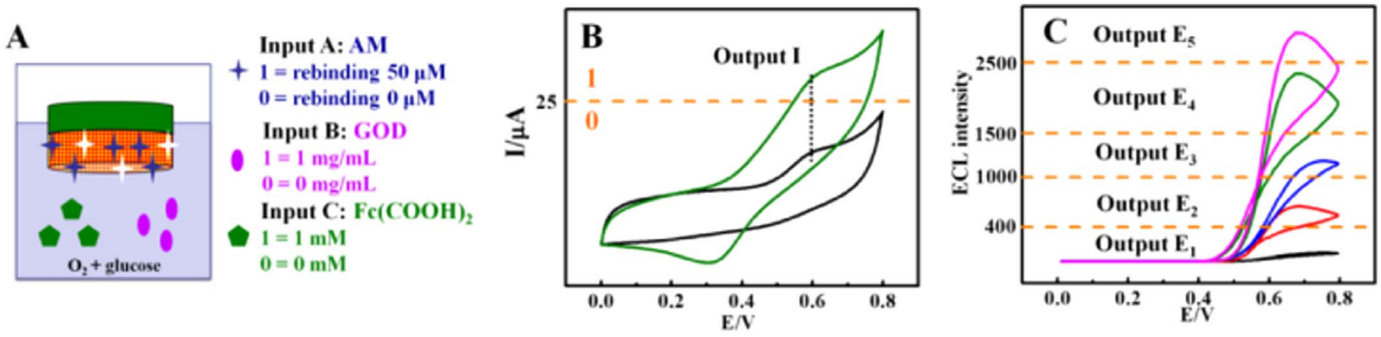

Scheme 2. Schematic definitions of (A) 3 inputs, (B) Output I and (C) Outputs E_1–E_5 on the working platform with AM-free MIP film electrodes in pH 8.0 buffers containing 2 μM glucose equilibrated with air. For the inputs, logic "0" and "1" values correspond to the absence and presence of the chemicals. For Outputs E_1–E_5, only the state of "1" was defined by the certain thresholds, otherwise it was defined as "0".

also be used to develop a 1-to-2 demultiplexer using Fc(COOH)$_2$ as the input (Input C) and AM as Address Input with Output I and E_5 as the 2 outputs. Particularly, the working platform was AM-free MIP film electrodes in the pH 8.0 solution containing 1 mg mL^{-1} GOD and 2 μM glucose (Fig. 4D, E and S10). When Address Input was set at the "0" state (AM-free MIP films), the binary state of Input C was transmitted directly to Output I. That is, the logic value "1" of Input C (with Fc(COOH)$_2$) would lead to the "1" state of Output I due to the higher CV response of Fc(COOH)$_2$ at the AM-free MIP film electrodes, while the "0" state of Input C (without Fc(COOH)$_2$) would result in Output I "0". Conversely, if the Address Input was switched to the "1" state (AM-rebinding MIP films), the binary state of Input C was directed to Output E_5. Namely, the logic value "1" of Input C (with Fc(COOH)$_2$) would lead to the "1" state of Output E_5 or largest ECL response (> 2500) because of the synergetic amplification of Fc(COOH)$_2$, GOD and AM, while the "0" state of Input C (without Fc(COOH)$_2$) would result in the "0" state of Output E_5 due to the lack of amplification from Fc(COOH)$_2$. The truth table of the 1-to-2 demultiplexer and the diagram of the equivalent switching device are demonstrated in Fig. 4D and E, and the logic circuit is shown in Fig. S11.

3.7. A ternary AND logic gate based on the same system

Logic computations based on multi-valued inputs and outputs rather than binary ones allow enhanced computational complexity (Orbach et al., 2015). For instance, a ternary logic gate defines 3 different states for input and output signals, which may correspond to logic values of 0, 1, and 2. Herein, based on the working platform of AM-free MIP film electrodes in pH 8.0 blank buffers in the absence of oxygen, a ternary AND logic gate was constructed. The addition of different chemicals was defined as Input 1, with null (nothing was added) as the "0" state, the addition of 1 mg mL^{-1} GOD and 2 μM glucose (GOD/glucose) as the "1" state, and the further addition of 1 μM Fc(COOH)$_2$ (GOD/glucose + Fc(COOH)$_2$) as the "2" state. Similarly, the operation with different steps was defined as Input 2, with null as the "0" state, equilibrated with air (O_2) as the "1" state, and the additional rebinding of AM (O_2 + AM) as the "2" state. The ECL peak signal was defined as Output E, with ECL ≤ 1000 as the "0" state, 1000 < ECL ≤ 2500 as the "1" state, ECL > 2500 as the "2" state, with 1000 and 2500 as the two thresholds. All 9 possible combinations of the two ternary inputs and the corresponding ternary outputs are shown in Fig. 5C. The input combinations (0,0), (1,0) and (2,0) led to the "0" state of Output E, because under the anaerobic condition the ECL response of the system was very small. For the input combinations (0,1) and (0,2), the oxygen was present and the ECL signal became larger, especially with the rebinding of AM. However, the enhancement of ECL by AM was not strong enough, which still led to the "0" state of Output E. The 3 input combinations (1,1), (2,1) and (1,2) resulted in the "1" state of Output E because of the amplification of GOD/glucose, the synergetic enhancement of GOD/glucose and Fc(COOH)$_2$, and the synergetic amplification of GOD/glucose and AM, respectively, in the presence of oxygen. The input combination (2,2) exclusively resulted in the "2" state of Output E due to the synergetic amplification of AM, GOD/glucose and Fc(COOH)$_2$. According to these results, the ternary AND logic gate was established with the truth table and the corresponding logic circuit in Fig. 5A and B.

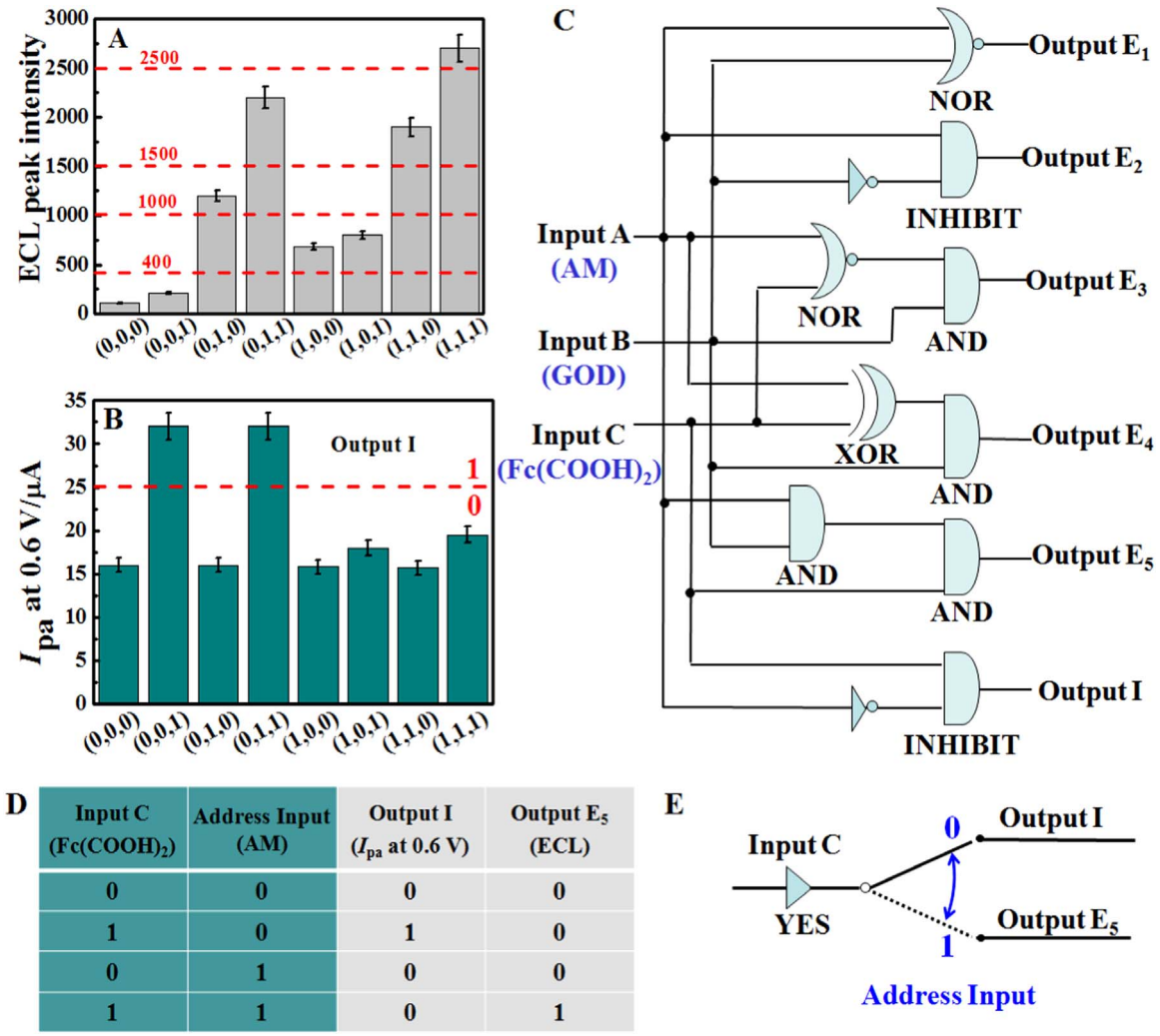

D

Input C (Fc(COOH)$_2$)	Address Input (AM)	Output I (I_{pa} at 0.6 V)	Output E_5 (ECL)
0	0	0	0
1	0	1	0
0	1	0	0
1	1	0	1

Fig. 4. (A) ECL peak intensity at 0.7 V and (B) CV I_{pa} at 0.6 V for different combinations of the 3 inputs of AM, GOD and Fc(COOH)$_2$. The thresholds were marked by dashed lines. The error bars represent the standard deviation of 3 repeated measurements. (C) Logic circuit for the 3-input/6-output logic gate system controlled by AM, GOD and Fc(COOH)$_2$. (D) Truth table and (E) the diagram of the equivalent switching device for the 1-to-2 demultiplexer.

4. Conclusions

In the present work, AM-PPY/PL MIP films were electropolymerized on the surface of Au electrodes, and the solid-state ECL responses were observed for the system and could be enhanced by AM rebinding, the addition of GOD/glucose and/or Fc(COOH)$_2$ in solution. Based on the same platform, a binary 3-input/6-output logic circuits, some non-Boolean logic devices, and a ternary AND logic gate were designed and developed. This work demonstrated some novel and unique characteristics: (1) The study combined MIP, solid-state ECL and enzymatic reaction together to fabricate biomolecular logic circuits and devices for the first time. (2) A more complicated ternary biocomputing logic gate was successfully constructed. (3) AM acted not only as the template in the MIP films, but also as the promoter to enhance the ECL response of PL in the films. (4) Both ECL and CV signals could be obtained simultaneously by the same instrument, and the intensity level of ECL was dependent on the different mechanisms, which greatly increased the number of outputs. The present system opened a new way

A

Output		Input 2		
		0 (null)	1 (O_2)	2 (O_2 + AM)
Input 1	0 (null)	0	0	0
	1 (GOD/glucose)	0	1	1
	2 (GOD/glucose + Fc(COOH)$_2$)	0	1	2

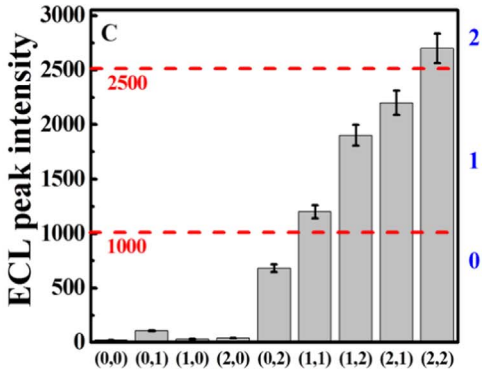

Fig. 5. (A) Truth table for the ternary AND logic gate. (B) Logic gate for the ternary AND logic gate. (C) ECL peak intensity at 0.7 V for different combinations of the two ternary inputs. The thresholds were marked by dashed lines. The error bars represent the standard deviation of 3 repeated measurements.

to develop complicated biomolecular logic system, and showed great potential for further expansion and extension. For example, the system could be easily extended by replacing AM with other template molecules for MIP, or by selecting other ECL promoter rather than Fc $(COOH)_2$, or by choosing other H_2O_2-producing enzymatic system instead of GOD/glucose. All these demonstrated the great flexibility and expansibility of the system.

Acknowledgments

The financial support from the National Natural Science Foundation of China (NSFC 21105004) and the Major Research Plan of NSFC (21233003) is gratefully acknowledged.

Appendix A. Supporting information

Supplementary data associated with this article can be found in the online version at http://dx.doi.org/10.1016/j.bios.2017.09.023.

References

Andreasson, J., Pischel, U., 2015. Chem. Soc. Rev. 44, 1053–1069.
Chantada-Vazquez, M.P., Sanchez-Gonzalez, J., Pena-Vazquez, E., Tabernero, M.J., Bermejo, A.M., Bermejo-Barrera, P., Moreda-Pineiro, A., 2016. Anal. Chem. 88, 2734–2741.
Chen, L., Xu, S., Li, J., 2011. Chem. Soc. Rev. 40, 2922–2942.
Chen, L., Zeng, X., Si, P., Chen, Y., Chi, Y., Kim, D.-H., Chen, G., 2014. Anal. Chem. 86, 4188–4195.
de Silva, A.P., Uchiyama, S., 2007. Nat. Nano 2, 399–410.
de Silva, A.P., Gunaratne, H.Q.N., McCoy, C.P., 1993. Nature 364, 42–44.
Erbas-Cakmak, S., Bozdemir, O.A., Cakmak, Y., Akkaya, E.U., 2013. Chem. Sci. 4, 858–862.
Erdossy, J., Kassa, E., Farkas, A., Horvath, V., 2017. Anal. Methods 9, 4496–4503.
Fu, X., Gu, Z., Lu, Q., Liao, J., Chen, S., 2016. RSC Adv. 6, 13217–13223.
Gao, R.-R., Yao, T.-M., Lv, X.-Y., Zhu, Y.-Y., Zhang, Y.-W., Shi, S., 2017. Chem. Sci. 8, 4211–4222.
Gui, R., Jin, H., Liu, X., Wang, Z., Zhang, F., Xia, J., Yang, M., Bi, S., 2014. Chem. Commun. 50, 14847–14850.
Guz, N., Halamek, J., Rusling, J.F., Katz, E., 2014. Anal. Bioanal. Chem. 406, 3365–3370.
He, K., Li, Y., Xiang, B., Zhao, P., Hu, Y., Huang, Y., Li, W., Nie, Z., Yao, S., 2015. Chem. Sci. 6, 3556–3564.
He, Y., Chen, Y., Li, C., Cui, H., 2014. Chem. Commun. 50, 7994–7997.
Hu, L., Xu, G., 2010. Chem. Soc. Rev. 39, 3275–3304.
Katz, E., 2015. Curr. Opin. Biotechnol. 34, 202–208.
Kim, D.-M., Moon, J.-M., Lee, W.-C., Yoon, J.-H., Choi, C.S., Shim, Y.-B., 2017. Biosens. Bioelectron. 91, 276–283.
Kubo, H., Saitoh, M., Murase, S., Inomata, T., Yoshimura, Y., Nakazawa, H., 1999. Anal. Chim. Acta 389, 89–94.
Li, J., Li, S., Wei, X., Tao, H., Pan, H., 2012. Anal. Chem. 84, 9951–9955.
Lian, W., Yu, X., Wang, L., Liu, H., 2015. J. Phys. Chem. C 119, 20003–20010.
Ling, Y., Gao, Z.F., Zhou, Q., Li, N.B., Luo, H.Q., 2015. Anal. Chem. 87, 1575–1581.
Liu, S., Wang, L., Lian, W., Liu, H., Li, C.-Z., 2015a. Chem. Asian J. 10, 225–230.
Liu, S., Li, M., Yu, X., Li, C.-Z., Liu, H., 2015b. Chem. Commun. 51, 13185–13188.
Manesh, K.M., Halamek, J., Pita, M., Zhou, J., Tam, T.K., Santhosh, P., Chuang, M.-C., Windmiller, J.R., Abidin, D., Katz, E., Wang, J., 2009. Biosens. Bioelectron. 24, 3569–3574.
Moon, J.-M., Kim, D.-M., Kim, M.H., Han, J.-Y., Jung, D.-K., Shim, Y.-B., 2017. Biosens. Bioelectron. 91, 128–135.
Orbach, R., Lilienthal, S., Klein, M., Levine, R.D., Remacle, F., Willner, I., 2015. Chem. Sci. 6, 1288–1292.
Park, K.S., Jung, C., Park, H.G., 2010. Angew. Chem. Int. Ed. 49, 9757–9760.
Privman, M., Tam, T.K., Pita, M., Katz, E., 2009. J. Am. Chem. Soc. 131, 1314–1321.
Pu, F., Ren, J., Yang, X., Qu, X., 2011. Chem. Eur. J. 17, 9590–9594.
Ran, X., Pu, F., Ren, J., Qu, X., 2014. Small 10, 1500–1503.
Sadki, S., Schottland, P., Brodie, N., Sabouraud, G., 2000. Chem. Soc. Rev. 29, 283–293.
Sato, Y., Sawaguchi, T., Mizutani, F., 2001. Electrochem. Commun. 3, 131–135.
Sato, Y., Kato, D., Niwa, O., Mizutani, F., 2005. Sens. Actuators B 108, 617–621.
Shi, W., Fu, Y., Li, Z., Wei, M., 2015. Chem. Commun. 51, 711–713.
Stojanovic, M.N., Mitchell, T.E., Stefanovic, D., 2002. J. Am. Chem. Soc. 124, 3555–3561.
Tan-Phat, H., Pieta, P., D'Souza, F., Kutner, W., 2013. Anal. Chem. 85, 8304–8312.
Ton, X.-A., Acha, V., Bonomi, P., Bui, B.T.S., Haupt, K., 2015. Biosens. Bioelectron. 64, 359–366.
Wang, X., Yang, Y., Gao, H., 2014. J. Lumin. 156, 229–234.
Wei, S., Liu, Y., Hua, T., Liu, L., Wang, H., 2014. J. Appl. Polym. Sci. 131.
Wei, X., Xiao, C., Liu, C., Wang, K., Tu, Y., 2014. Electroanalysis 26, 807–814.
Willner, I., Shlyahovsky, B., Zayats, M., Willner, B., 2008. Chem. Soc. Rev. 37, 1153–1165.
Wu, B., Wang, Z., Xue, Z., Zhou, X., Du, J., Liu, X., Lu, X., 2012. Analyst 137, 3644–3652.
Xia, F., Zuo, X., Yang, R., White, R.J., Xiao, Y., Kang, D., Gong, X., Lubin, A.A., Vallee-Belisle, A., Yuen, J.D., Hsu, B.Y.B., Plaxco, K.W., 2010. J. Am. Chem. Soc. 132, 8557–8559.
Xue, X., Wei, Q., Wu, D., Li, H., Zhang, Y., Feng, R., Du, B., 2014. Electrochim. Acta 116, 366–371.
Yao, H., Hu, N., 2009. J. Phys. Chem. B 113, 16021–16027.